Supporting Information

Adjusting anion-solvent dipole interactions in ether-based electrolytes for wide temperature range applications of sodium-ion batteries

*Yixing Shen[ab], Jipeng Xu[c], Yana Li[d], Shuzhi Zhao[a], Haiying Che[b], Jabeen Maher[b], Xuan Wang[c], Yunlong Zhang[ab], Jiafang Wu[e], Jingkun Li[c], Cheng Lian[c], Zi-Feng Ma[*abd]*

[a]*Shanghai Electrochemical Energy Devices Research Center, Department of Chemical Engineering, Shanghai Jiao Tong University, Shanghai 200240, China*

[b]*Zhejiang Natrium Energy Co., Ltd, Shaoxing, Zhejiang, 312300, China*

[c]*School of Chemical Engineering, East China University of Science and Technology, Shanghai, 200237, China*

[d]*Shaoxing Research Institute of Renewable Energy and Molecular Engineering, Shanghai Jiao Tong University, Shaoxing, Zhejiang, 312300, China*

[e]*Nanjing Normal University, Nanjing, Jiangsu, 210023, China*

**Address correspondence to: zfma@sjtu.edu.cn*

Experiments

Materials and Electrolyte preparation

The following chemicals were purchased: sodium hexafluorophosphate ($NaPF_6$, Adamas), Lithium difluoro(oxalato)borate (LiDFOB, Adamas), diglyme (G2, Adamas), ethyl methyl carbonate (EMC, Adamas), propylene carbonate (PC, Adamas), fluorinated ethylene carbonate (FEC, Energy Chemical), sodium tetrafluoroborate ($NaBF_4$, Aladdin, 99.9% purity), 1,3-propanesulfolactone (PS, Aladdin), propylene 1,3-sulfonic acid lactone (PST, Aladdin), hard carbon (HC, Kuraray). Additionally, industrial-grade $NaBF_4$ (98% purity) was purchased from Jinan Xinshun Chemical Co., Ltd. Both $NaBF_4$ and $NaPF_6$ were dried under vacuum at 100 ℃ for 12 h before use.

The 1M-BG2-LB, 1M-BG2, 0.5M-BG-LB, and 0.5M-BG electrolytes were prepared by dissolving 1, 1, 0.5, 0.5 mol $NaBF_4$ in 1 L DEGDME solvent, respectively. The 1M-BG2-LB and 0.5M-BG-LB electrolytes were prepared by adding 0.15 mol LiDFOB as an additive into the corresponding electrolytes (Table S2). The only difference is that the 1M-BG2-LB used industrial-grade $NaBF_4$ salt (98% purity), compared to the 1M-BG2-LB (99.9% battery grade $NaBF_4$ salt) using the 99.9% $NaBF_4$. The 1M-$NaPF_6$-comercial electrolyte was prepared by adding 1 mol $NaPF_6$ (167.95g), 1 wt% FEC (12.87g), 1% PS (12.87g), and 1% PST (12.87g) into 1 L PC/EMC (4:6 by volume) solvent blend and stirring until a clear solution formed.

Preparation of electrode

Electrodes used in coin cells: $Na[Ni_{1/3}Fe_{1/3}Mn_{1/3}]O_2$ (NFM) and $Na_3V_2(PO_4)_3$ (NVP) cathodes were prepared by slurry-coating in a mass ratio of 80 (NFM or NVP):

10 (PVDF) : 10 (Super-P carbon(using 1-methyl-2-pyrrolidone solvent. The mass loading of the NFM cathode was around 1.8~2.0 mg cm^{-2}. Similarly, $Na_{4/3}Fe_{3/2}(PO_4)_{2/1}P_2O_7$ (NFPP) cathode was prepared in a mass ratio of 85 (NFPP) : 8 (PVDF) : 7 (Super-P carbon) with the NFPP loading of 3.8~4.0 mg cm^{-2}. The hard carbon (HC) anode was fabricated in a mass ratio of 80 (HC): 10 (PVDF) : 10 (Super-P carbon) with the HC loading of 0.8~0.9 mg cm^{-2}. The N/P capacity ratio in the NFM||HC full cells was 1.2. All the symmetric-, half- and full-cells used a PP/PE-based separator and were assembled in a form of CR2016.

Electrodes used in pouch cells: The NFPP cathode consisted by weight of 93% NFPP: 4% PVDF, and 3% Super-P carbon, with an NFPP loading of approximately 13.5 mg cm^{-2}. The HC anode consisted of 95% HC, 1.5% CMC, 2.5% SBR, and 1% Super-P carbon. Before use, the CMC and SBR binders were dispersed in H_2O, and the resultant HC anode had an HC loading of around 6 mg cm^{-2}. The N/P capacity ratio in the NFPP||HC pouch cells was 1.2. All cells were assembled in an Ar-filled glovebox (O_2 ＜0.1 ppm, H_2O ＜0.1 ppm).

Material characterizations

The reaction products of water were analyzed by XRD (HAOYUAN DX-2700BH). Microscopic images were obtained using scanning electron microscopy (HITACHI SU3800), transmission electron microscopy (Thermo Scientific Talos F200X G2), and atomic force microscope (Oxford MFP-3D). Spectroscopy analyses were conducted using Raman spectra (Renishaw inVia Qontor), Fourier transform infrared spectroscopy(SHIMAZU IRAffinity-1S), and nuclear magnetic resonance

(Bruker AVANCE NEO 700MHz). The surface chemistry of the cycled electrodes was characterized by XPS (SHIMADZU Kratos AXIS UltraDLD) and TOF-SIMS (ION TOF TOF SIMS 5-100).

Electrochemical measurements

Ionic conductivity of electrolytes was measured using a conductivity meter (Shanghai INESA Scientific Instrument Co.,Ltd DDS-307A). Electrochemical stability window, cyclic voltammogram (CV), and electrochemical impedance spectroscopy (EIS) were analyzed using an electrochemical workstation (Princeton VersaSTAT 4). Linear sweep voltammetry (LSV) was performed by sweeping the potential from the open-circuit voltage at ~2.5 V to 5.5 V at a scanning rate of 1 mV/s. EIS was measured over a frequency range of 10 mHz ~ 1 MHz. The CVs of the NFPP||Na half-cells were acquired at 0.1~1.0 mV/s within the voltage range of 2.0-4.0 V. The C rate was based on a current rate of 1C = 100 mA/g. The Na||Na symmetric cells were charged and discharged at 0.5 mA/cm^2 for a capacity of 0.5 mAh/cm^2.

Additional remarks

Electrochemical tests are conducted at 25 ℃ unless otherwise specified.

NFM||Na half cells were investigated to evaluate the high-voltage electrochemical performances of 1M-BG2-LB electrolyte. As shown in the Fig. S15, the 1M-BG2-LB electrolyte composed of battery-grade $NaBF_4$ salt (99.9% purity) retained 86.9% capacity after 400 cycles with 4.0 V cutoff voltage and an analogous capacity retention (87.1%) was obtained in 1M-BG2-LB electrolyte composed of low cost industrial-grade $NaBF_4$ salt (98% purity), confirming the strong tolerance of $NaBF_4$ salt to H_2O.

The 1M-BG2-LB cells deliver an initial discharge specific capacity of 139.8 mAh g^{-1}, leading to a capacity retention of 89.2% and a high average coulombic efficiency (CE, 99.8%) with a charge cut-off voltage of 4.2 V after 200 cycles at 1 C (Fig. S16a-b). A similar coulombic efficiency (CE, 99.5%) can still be maintained, result in a capacity retention of 81.1% after 200 cycles even with 4.3 V high cutoff voltage. To further evaluate the electrolyte designs, electrochemical performances of NFM||HC full cells were demonstrated with a charge cut-off voltage of 4.0 V (Fig. S16c-d). In contrast, The capacity retention of cells using 1M-BG2-LB electrolyte remain as 80.8% capacity retention after 200 cycles, far higher than that in commercial electrolytes (66.1%), exhibiting great potentials applied in high-voltage sodium batteries. The 1M-BG2-LB electrolyte also exhibits superior cycling stability compared to 1M-BG2 electrolyte in NVP||Na and NFPP||Na half cells (Fig. S16a-d).

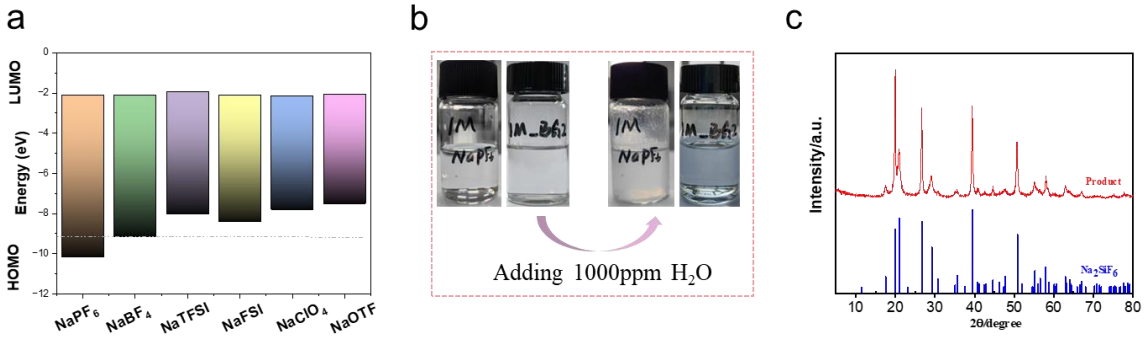

Fig. S1. (a) Lowest unoccupied molecular orbital (LUMO) and highest occupied molecular orbital (HOMO) energy levels of various sodium salts. (b) Water tolerance testing of different electrolytes. (c)XRD pattern of white by-products after adding 1000ppm H_2O in the commercial electrolyte (with 1M $NaPF_6$).

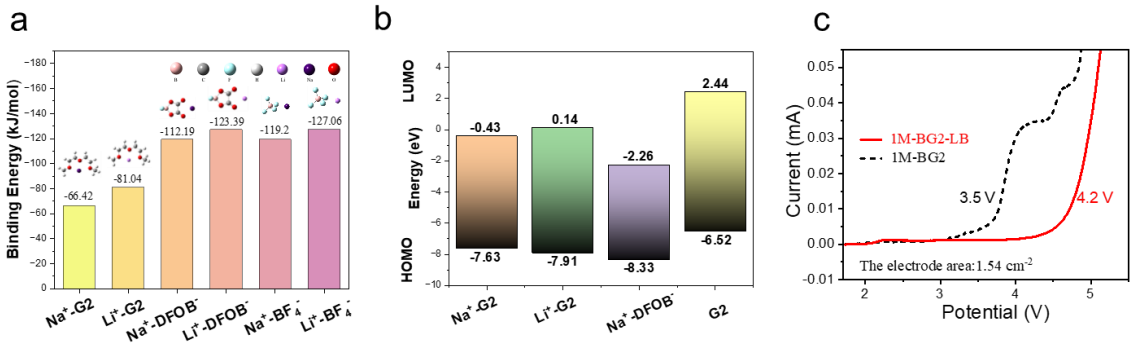

Fig. S2. (a) Binding energies of Na^+ and Li^+ with G2、BF_4^- and $DFOB^-$. (b) LUMO and HOMO levels of various coordination structures and free solvent. (c) Linear sweep voltammetry curves for various electrolytes at a scan rate of 1 mV s^{-1}.

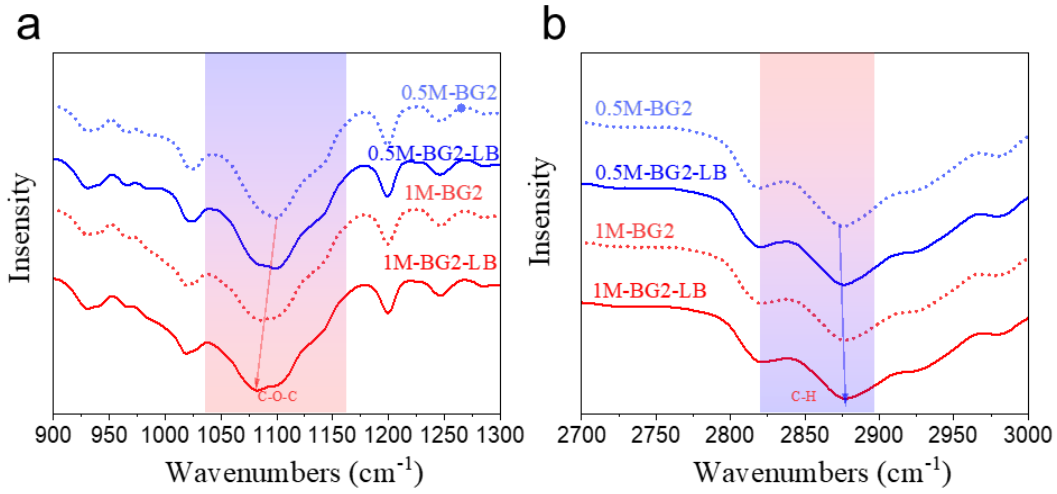

Fig. S3. (a) The FT-IR spectra of C-O-C and (b) C-H stretching mode in various electrolytes.

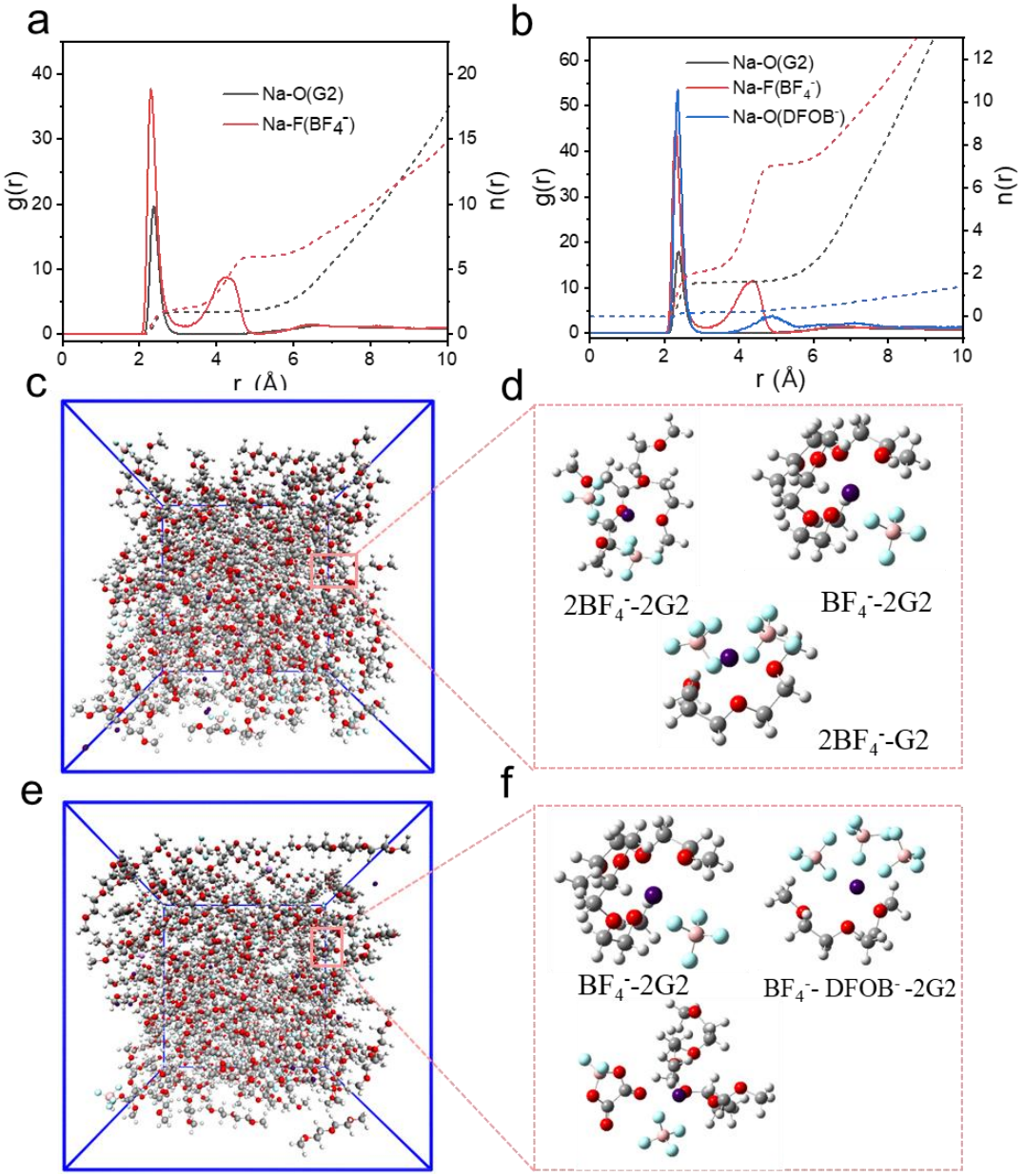

Fig. S4. Na^+ radical distribution functions (RDFs) from MD simulation of (a) 1M-BG2 electrolyte and (b) 1M-BG2-LB electrolyte. Snapshot and typical solvation structure obtained from MD simulation of (c, d) 1M-BG2 and (e, f) 1M-BG2-LB electrolyte.

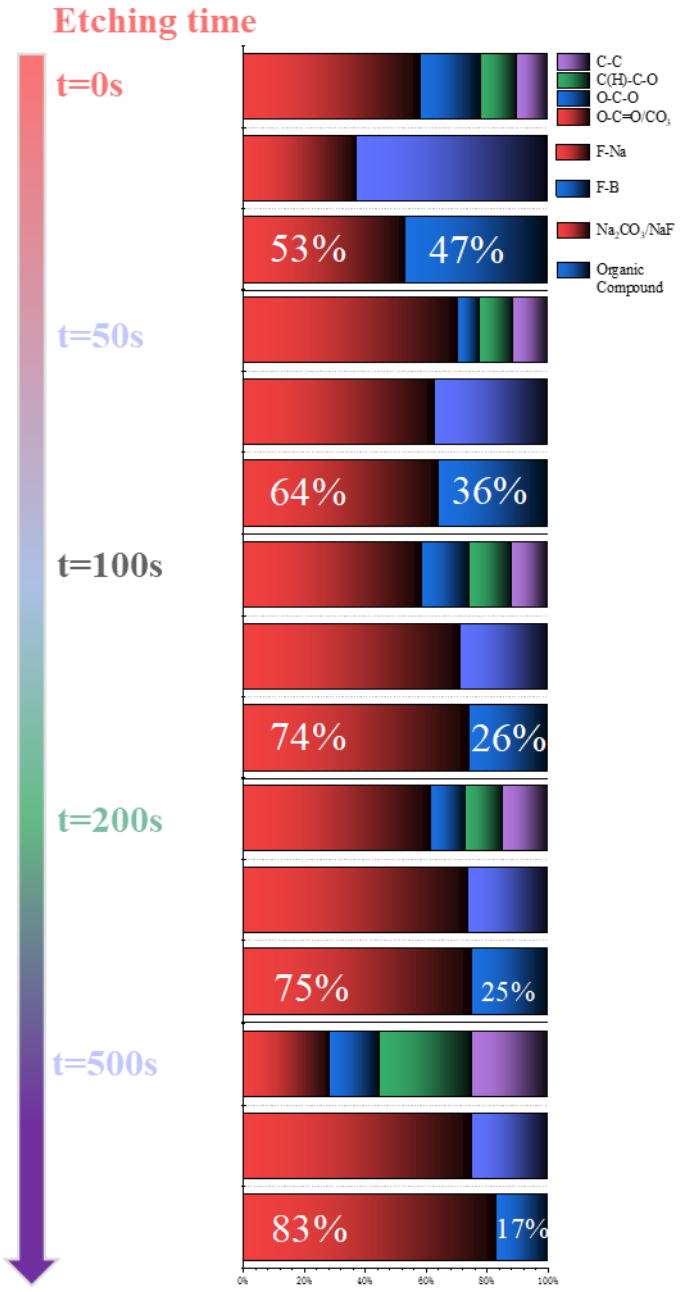

Fig. S5. Changes in various species according to XPS spectra on the Na electrode surface after 100 cycles in 1M-BG2-LB electrolyte, with Argon ion-beam sputtering time.

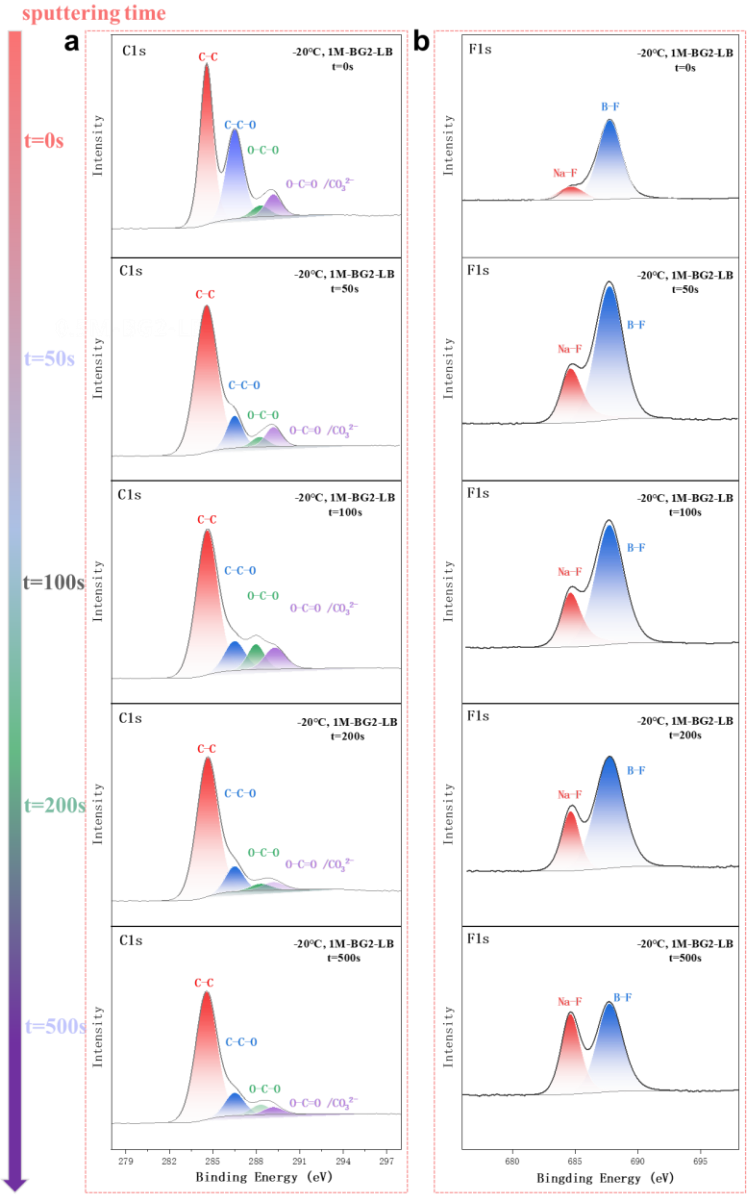

Fig. S6. Changes in XPS spectra of C1s (a) and F1s (b) on the Na electrode surface after 100 cycles (NFPP||Na cells) in 1M-BG2-LB electrolyte at -20 °C and 0.3C, with Argon ion-beam sputtering time.

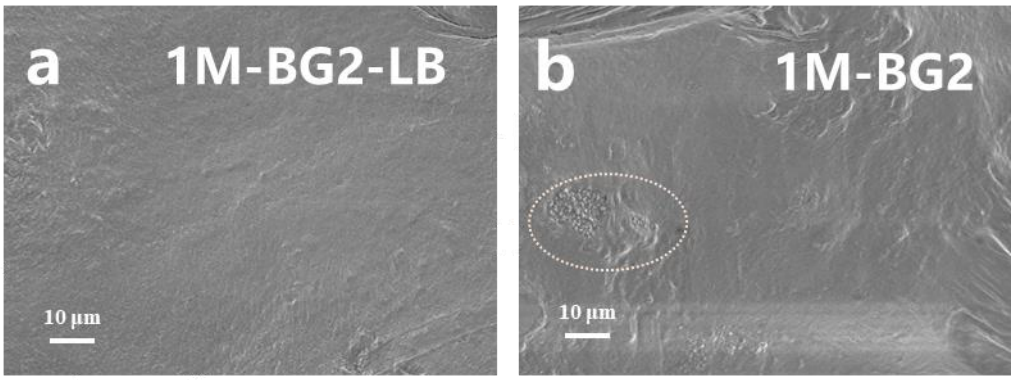

Fig.

Fig. S7. (a-b) SEM images of the Na electrode after 100 cycles in various electrolytes at -20 °C and 0.3C.

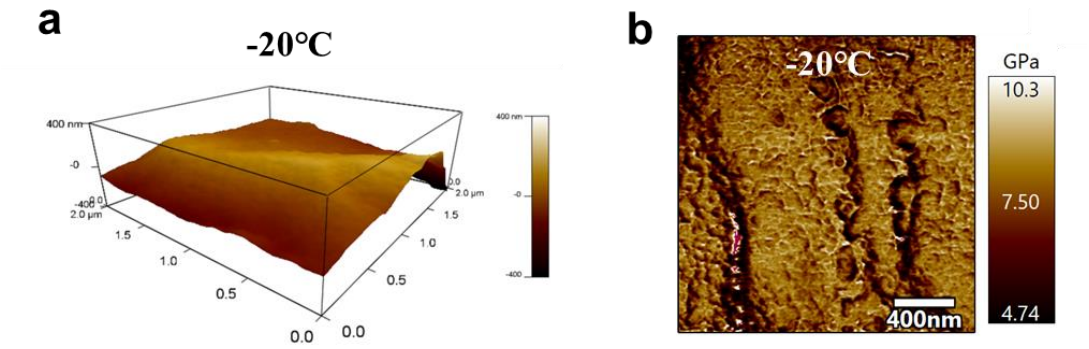

Fig. S8. (a) AFM 3D topographic images of the HC electrode cycled in 1M-BG2 electrolyte at -20 °C, (b) with the corresponding Young's modulus profiles.

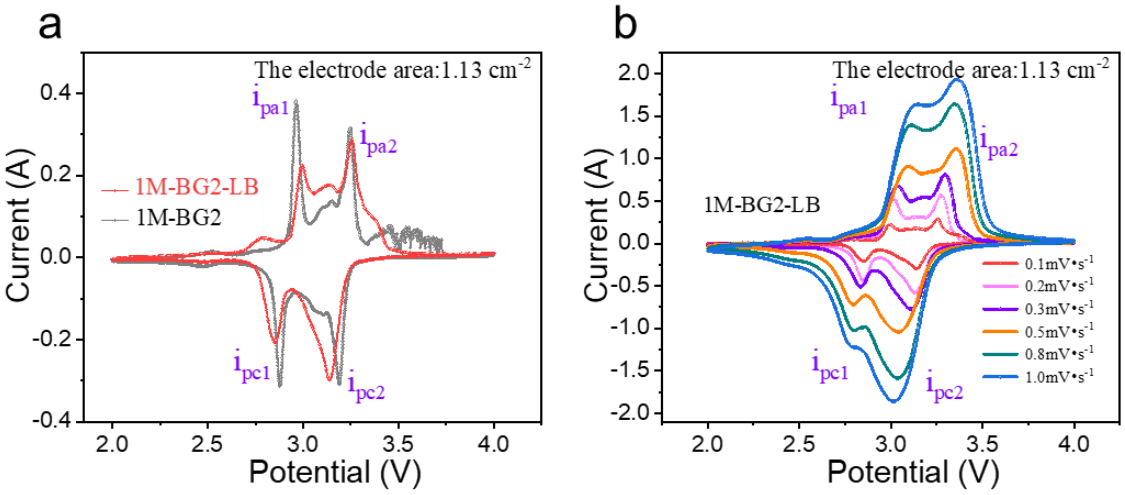

Fig. S9. (a) Cyclic voltammetry curves (NFPP||Na cells) for various electrolytes at a scan rate of 0.1 mV s^{-1}. (b) Cyclic voltammetry curves (NFPP||Na cells) for 1M-BG2-LB electrolyte at a scan rate of 0.1~1 mV s^{-1}.

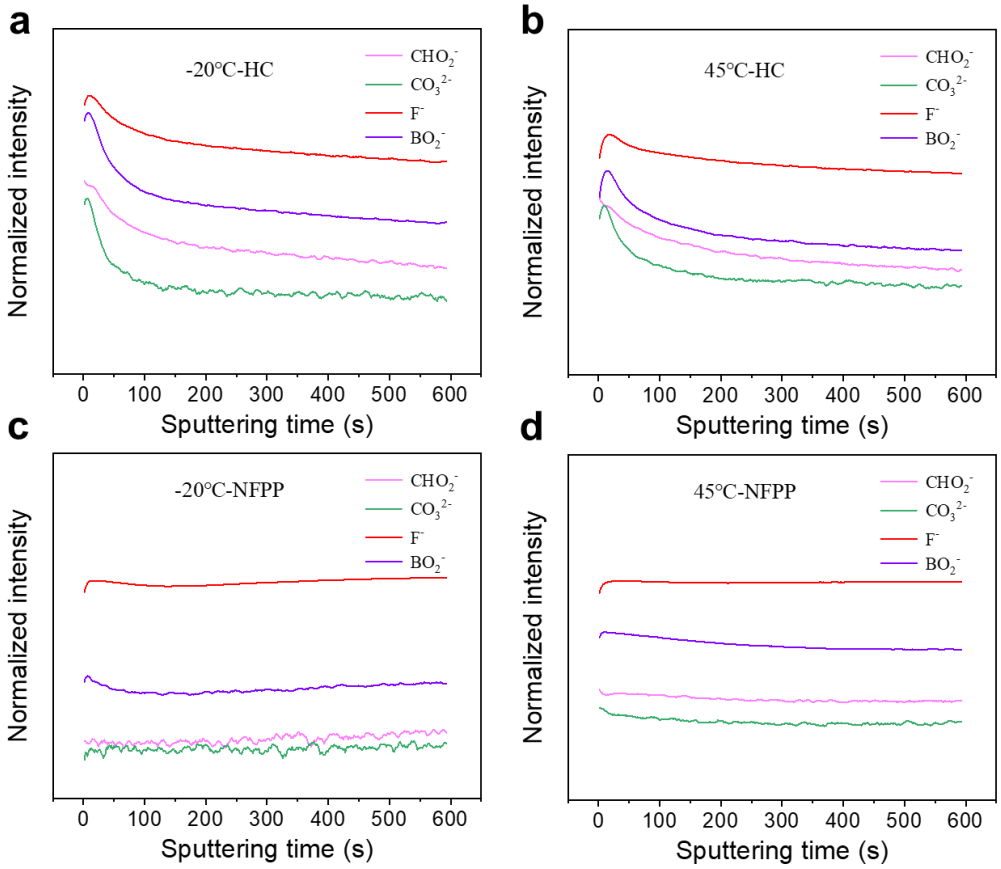

Fig. S10. Normalized TOF-SIMS depth profiles for CHO_2^-、CO_3^{2-}、F^- and BO_2^- secondary ions of SEIs on the HC electrode cycled in 1M-BG2-LB electrolyte at -20 °C (a) and 45 °C (b). Normalized TOF-SIMS depth profiles for CHO_2^-、CO_3^{2-}、F^- and BO_2^- secondary ions of CEIs on the NFPP electrode cycled in the 1M-BG2-LB electrolyte at -20 °C (c) and 45 °C (d).

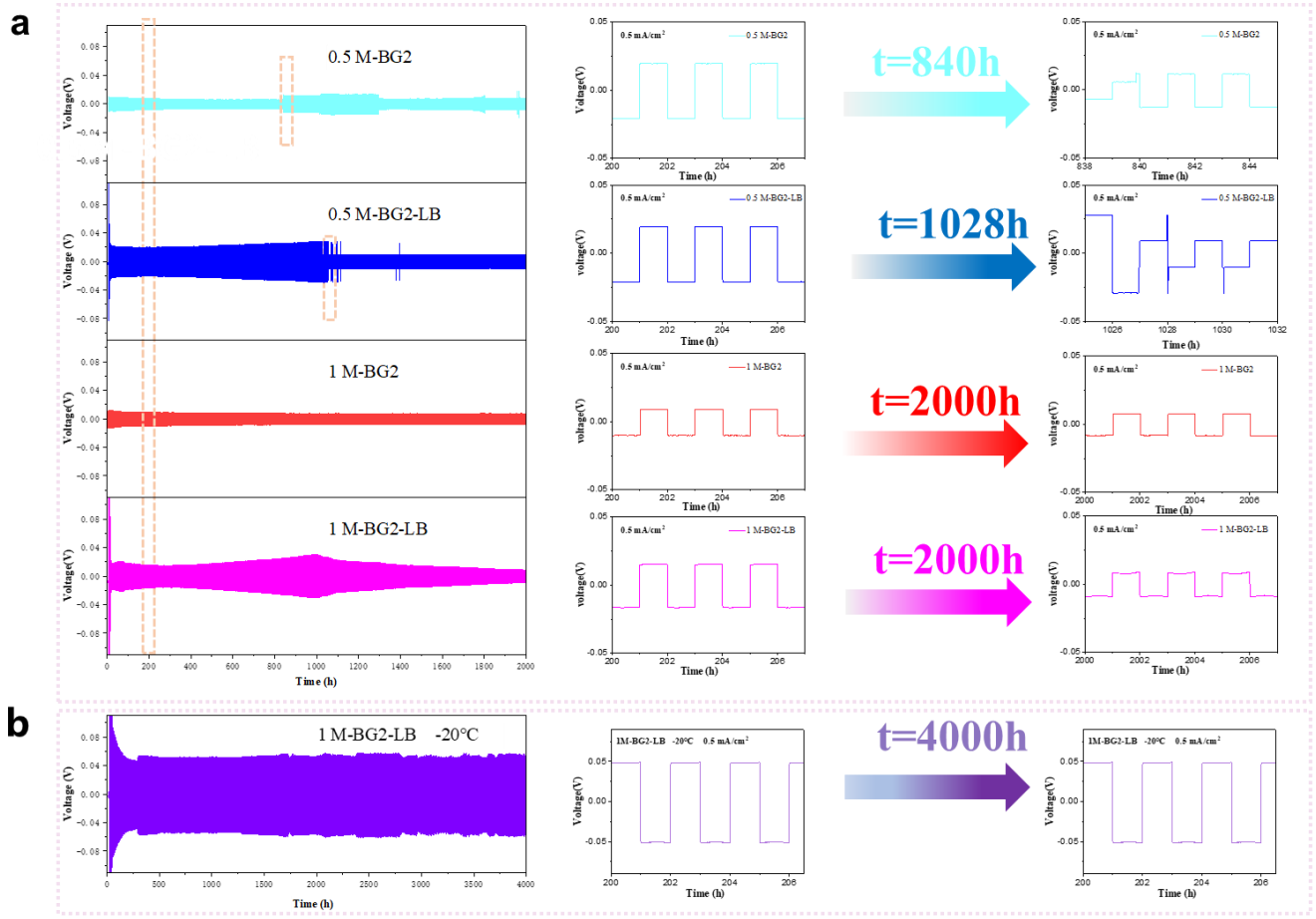

Fig. S11. (a) Cycling performance of Na||Na symmetrical cells with various electrolytes at 25 °C and a current density of 0.5 mA cm^{-2} with a capacity of 0.5 mAh cm^{-2}. (b) Cycling performance of Na||Na symmetrical cells with 1 M-BG2 electrolyte at -20 °C and a current density of 0.5 mA cm^{-2} with a capacity of 0.5 mAh cm^{-2}.

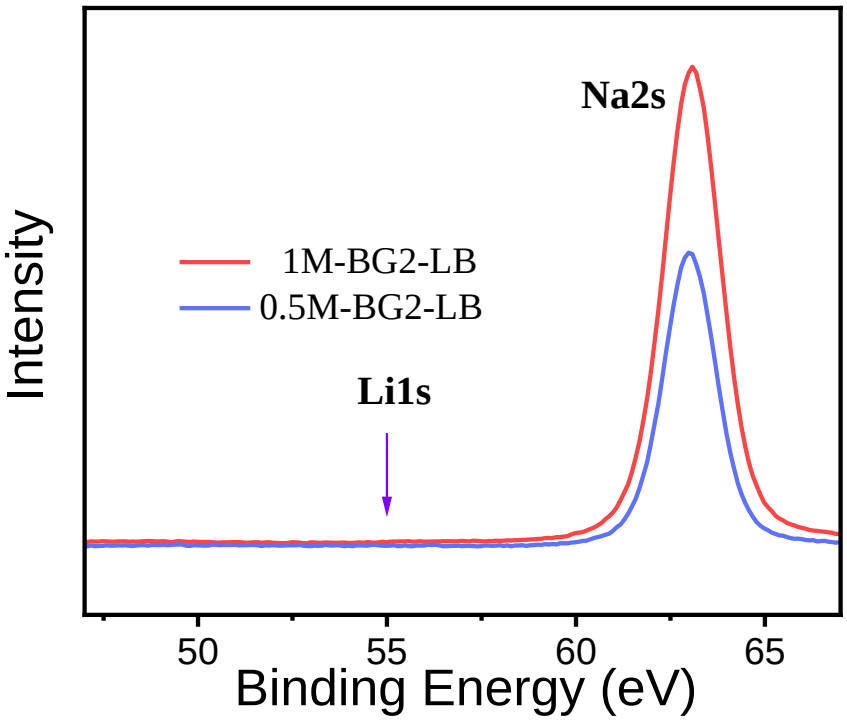

Fig. S12. XPS spectra on the Na metal electrodes cycled with Li^+ ions in the electrolytes.

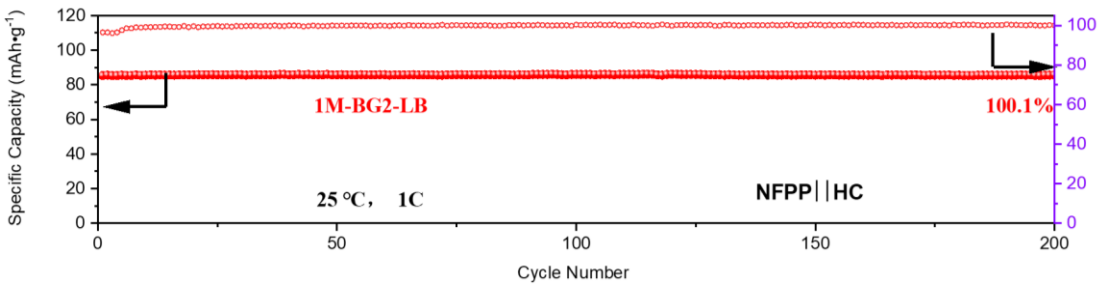

Fig. S13. Electrochemical performance of NFPP||HC pouch batteries: Long-term galvanostatic cycling at 25 °C under a current density of 1C.

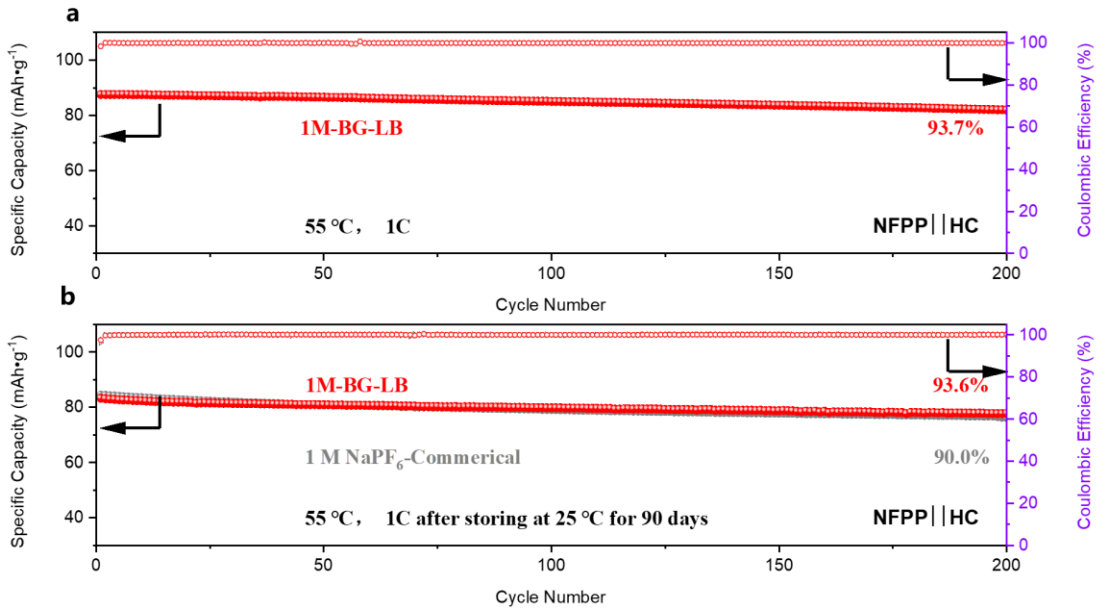

Fig. S14. Electrochemical performance of NFPP||HC pouch batteries (a) Long-term galvanostatic cycling at 55 °C under a current density of 1C and (b) after storing at 25 °C for 90 days.

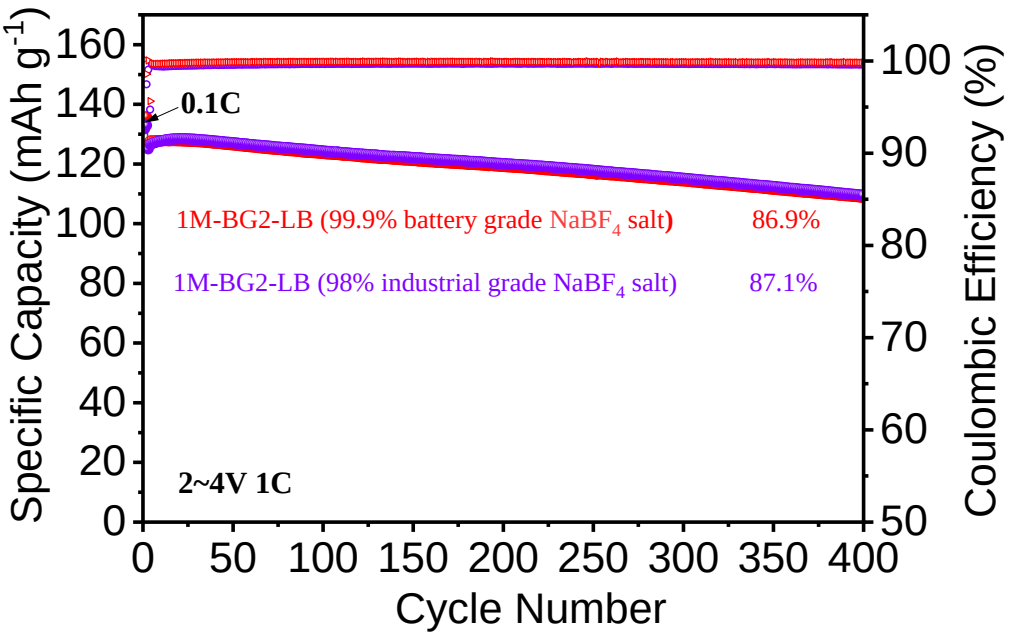

Fig. S15. Long-term galvanostatic cycling of NFM-Na half batteries with 4.0 V cutoff voltage in 1M-BG2-LB electrolyte at 25 °C, the current density is 0.1C for the initial 2 cycles and then 1C for the subsequent cycling.

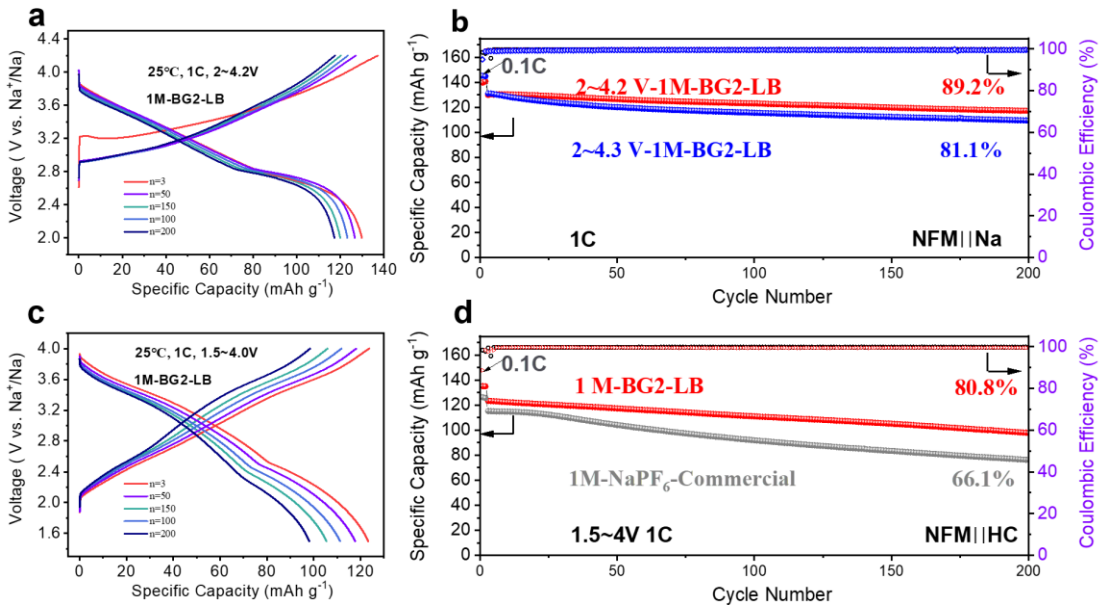

Fig. S16. (a) Galvanostatic charge/discharge voltage profiles and (b) Long-term galvanostatic cycling of NFM-Na half batteries in 1M-BG2-LB electrolyte at 25 °C, the current density is 0.1C for the initial 2 cycles and then 1C for the subsequent cycling. (c) Galvanostatic charge/discharge voltage profiles and (d) Long-term galvanostatic cycling of NFM-HC full batteries at 25 °C, the current density is 0.1C for the initial 2 cycles and then 1C for the subsequent cycling.

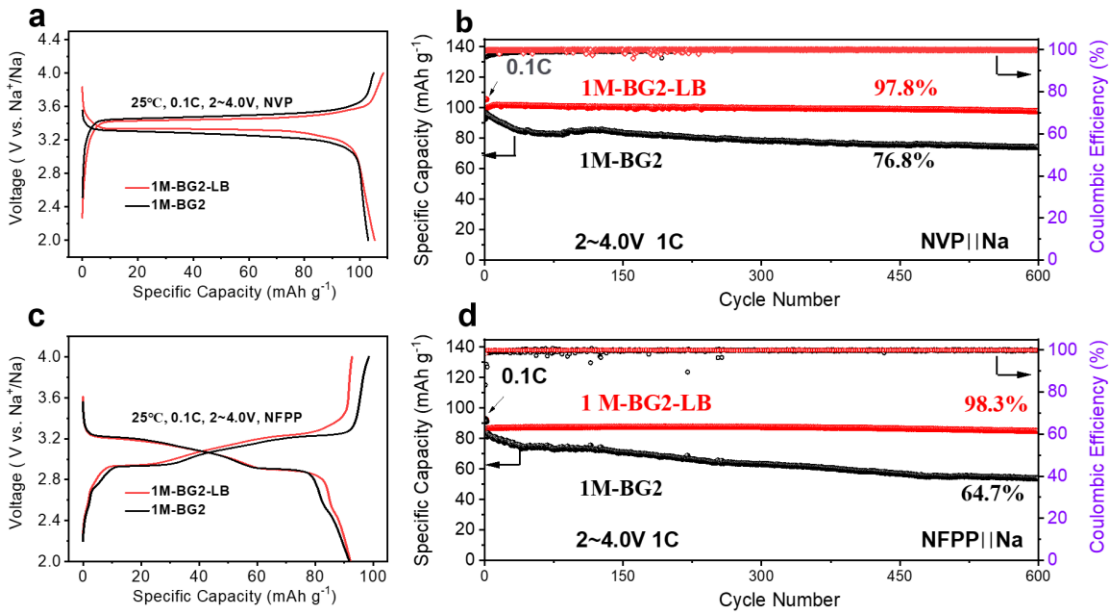

Fig. S17. Galvanostatic charge/discharge voltage profiles and Long-term galvanostatic cycling of NVP||Na (a, b) and NFPP||Na (c, d) half batteries in 1M-BG2-LB and 1M-BG2 electrolytes at 25 °C, the current density is 0.1C for the initial 2 cycles and then 1C for the subsequent cycling.

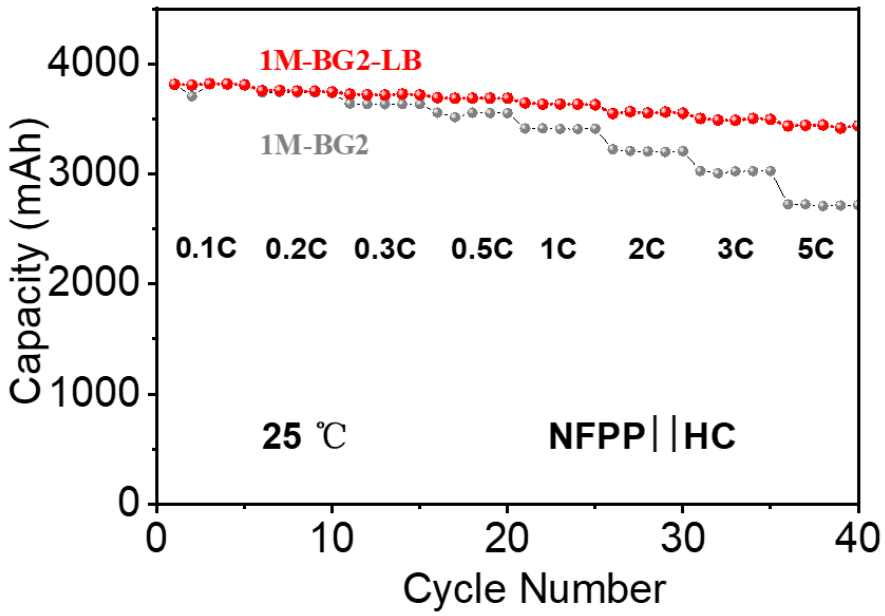

Fig. S18. Rate capability of NFPP||HC pouch batteries at 25 °C.

Table S1. The ratio of various solvation structures of BF_4^- and $DFOB^-$ anions in various electrolytes.

BF_4^-

Sample	SSIP (%)	CIP (%)	AGG (%)
0.5M-BG2-LB	45.3	18.8	35.8
0.5M-BG2	50.6	22.9	26.5
1 M-BG2-LB	29.8	26.8	43.4
1 M-BG2	37.8	22.8	39.0

$DFOB^-$

Sample	SSIP (%)	CIP (%)	AGG (%)
0.5M-BG2-LB	66.7%	30.2%	3.1%
0.5M-BG2			
1 M-BG2-LB	33.8%	63.7%	2.5%
1 M-BG2			

Table S2. Preparation of various electrolytes.

Sample	$NaBF_4$	G2	LiDFOB
0.5M-BG2-LB	0.5 mol	1L	0.15 mol
0.5M-BG2	0.5 mol	1L	-
1 M-BG2-LB	1.0 mol	1L	0.15 mol
1 M-BG2	1.0 mol	1L	-

Table S3. The conductivity of the four electrolytes at different temperatures (mS/cm).

Sample	25°C	-20°C	-40°C
1M-BG2-LB	2.58	2.06	1.75
1M-BG2	0.45	0.36	0.27
0.5M-BG2-LB	0.66	0.41	0.28
0.5M-BG2	0.39	0.30	0.18

Table S4. Comparison with excellent wide temperature range electrolytes reported in literature.

Working Temperature	Capacity Retention in high Temperature	Capacity Retention in low Temperature	Cycling performance of symmetrical cells in low Temperature	Journal
NVPF‖HC (-25~70°C)	93.0% (50°C, 1000 cycles)	94.0% (-25°C, 500 cycles)	-	J. Am. Chem. Soc,2024, 146 ,7295-7304[1]
NVP‖Na (-60~0°C)	-	96.2% (-20°C, 1000 cycles)	900h (-20°C, 3.0 mA/cm^2)	Energy Storage Mater., 2022, 50, 47-54[2]
NVPF‖NTO (-60~-20°C)	-	96.5% (-20°C, 10000 cycles)	-	Nano Energy, y 2022, 102, 107693[3]
Na‖HC (-60~55°C)	73.5% (55°C, 250 cycles)	87.0% (-40°C, 700 cycles)	-	Nat. Commun., 2024, 15, 8866[4]
NFM‖Na (-35~45°C)	87.1% (45°C, 250 cycles)	Only charge-discharge curves	-	ACS Energy Lett. 2024, 9, 4655−4665[5]
NFPP‖HC (-20~60°C)	96.7% (60°C, 60 cycles)	Only charge-discharge curves	-	Energy Storage Mater., 2024, 73, 103805[6]
NVP‖Na (-45~60°C)	84.7% (60°C, 3000 cycles)	95.1% (-25°C, 500 cycles)	-	Angew. Chem. Int. Ed., 2024, 136, e202401051[7]
NFM‖Na (-20~60°C)	93.0% (25°C, 150 cycles)	92.5% (-20°C, 150 cycles)	1300h (25°C, 0.26 mA/cm^2)	Adv. Funct. Mater. 2024, 34, 2312295[8]
NVP‖Na (-20~60°C)	85.7% (60°C, 60 cycles)	~99.0% (-20°C, 60 cycles)	3000h (30°C, 0.20 mA/cm^2)	Adv. Funct. Mater. 2024, 2407713[9]
NVP‖Na (-35~60°C)	92.2% (60°C, 250 cycles)	~99.0% (-20°C, 3 cycles)	750h (25°C, 0.20 mA/cm^2)	Angew. Chem. Int. Ed. 2024, 63, e202402245[10]
NFPP‖HC (-50~55°C)	87.8% (45°C, 1000 cycles) 93.7% (55°C, 200 cycles)	98.3% (-20°C, 500 cycles)	2000h (25°C, 0.50 mA/cm^2) 4000h (-20°C, 0.50 mA/cm^2)	This work

References：

[1] H. Liang, H. Liu, X. Zhao, Z. Gu, J. Yang, X. Zhang, Z. Liu, Y. Tang, J. Zhang and X. Wu*, J. Am. Chem. Soc, 2024, 146, 7295-7304.

[2] Y. Ding, S. Dong, Q. Zhu, M. Tang, Y. Wang, Y. Bi,R. Sun, Z. Wang and H. Wang*, Energy Storage Mater., 2022, 50, 47-54.

[3] Y. Zheng, M. Sun, F. Yu, L. Deng, Y. Xia, Y. Jiang, L. Que, L. Zhao and Z. Wang*, Nano Energy, 2022, 102, 107693.

[4] M. Wang, L. Yin, M. Zheng, X. Liu, C. Yang, W. Hu, J. Xie, R. Sun, J. Han, Y. You* and J. Lu*, Nat. Commun., 2024, 15, 8866.

[5] M. Ma, B. Chen, Y Tu and H Pan*, ACS Energy Lett. 2024, 9, 4655−4665.

[6] E. Li, L. Liao, J. Huang, T. Lu, B. Dai, K. Zhang, X. Tang, S. Liu, L. Lei, D. Yin, J. Teng and J. Li, Energy Storage Mater., 2024, 73, 103805.

[7] M. He, L. Zhu, G. Ye, Y. An, X. Hong, Y. Ma, Z. Xiao, Y. Jia and Q. Pang*, Angew. Chem. Int. Ed., 2024, 136, e202401051.

[8] Y. Liu, S. Lu, Z. Wang, J. Xu*, S. Weng, J. Xue, H. Tu, F. Zhang, L. Liu, Y. Gao, H. Li, J. Zheng*and X. Wu*, Adv. Funct. Mater. 2024, 34, 2312295.

[9] Z. Yang, H. Jiang, X. Li, X. Liang, J. Wei, Z. Xie, B. Tang*, Y. Zhang and Z. Zhou*, Adv. Funct. Mater. 2024, 2407713.

[10] X. Guo, Z. Xie, R. Wang, J. Luo, J. Chen, S. Guo,G. Tang, Y. Shi and W. Chen*, Angew. Chem. Int. Ed. 2024, 63, e202402245.